

BUTP-96/10, hep-ph/9604217

Scattering Lengths and Medium and High Energy Scattering

B. Ananthanarayan

P. Buttiker

Institut für theoretische Physik

Universität Bern, CH-3012 Bern, Switzerland

Abstract

Medium and high energy absorptive parts contribute to dispersive expressions for D-wave scattering lengths, a_2^0 and a_2^2 . For the model employed by Basdevant, Frogatt and Peterson we find the D-wave driving term contributions to the D-wave scattering lengths are $1.8 \cdot 10^{-4}$ to a_2^0 and $0.4 \cdot 10^{-4}$ to a_2^2 , roughly 10% and 30% of their respective central experimental values. Inequivalent sets of sum rules are used as a compelling test of the consistency of the model for which crossing symmetry is not guaranteed. Results for the F-wave scattering length a_3^1 are presented, completing the recent Roy equation analysis of scattering in the range for a_0^0 favored by standard chiral perturbation theory.

1 Introduction

The Roy equations [1, 2], a system of integral equations for physical region partial wave amplitudes based on (fixed t -) dispersion relations, provide the necessary tools besides analyticity, unitarity and crossing [3, 4] for the analysis of low energy S- and P-wave scattering [5, 6]. Best fits to the experimental data and Roy equations for the two lowest waves yield $a_0^0 = 0.26 \pm 0.05$ [7]. Chiral perturbation theory, the low-energy limit of the strong interactions [8] among other things predicts scattering lengths as well as higher threshold parameters of $\pi\pi$ scattering. Standard one-loop chiral perturbation theory predicts, for instance, $a_0^0 = 0.20 \pm 0.01$ [9]. A generalized version [10] predicts larger values for a_0^0 and is related to the question of small quark condensates in QCD; two-loop $\pi\pi$ scattering amplitudes in this framework were recently presented [11] in addition to a field-theoretic calculation in the standard chiral perturbation theory [12].

A revival of interest in $\pi\pi$ scattering and the underlying theory and assumptions has been recently witnessed [13]. Furthermore, the method of Roy equation analysis of Basdevant, Froggatt and Petersen (BFP) [5, 6] has been reimplemented in order to analyse $\pi\pi$ scattering data with a_0^0 chosen to lie in the range favored by standard chiral perturbation theory [14]. The end product of the BFP method is the availability of a parametric representation for the absorptive parts of the three lowest waves f_0^0 , f_0^2 and f_1^1 in the region

4 s 110. However the Roy equations extend over the entire energy domain of scattering and involves all partial waves: the information content of these is modeled in terms of the known resonances such as what is now called the $f_2(1270)$ [15] (an $I = 0, l = 2$ state) [but we will refer to this as f_0 in accordance with BFP] and in terms of Regge phenomenology which then supply the driving terms to the Roy equations of the S- and P-waves. BFP appeal to such a model and present simple polynomial fits to the driving terms. The availability of the polynomial fits to the S- and P-wave driving terms yields sharp predictions for certain (combinations) of S- and P-wave threshold parameters that are correlated with the choice of a_0^0 that was input in the recent Roy equation analysis [14].

Roy equations may also be written down for the higher waves and solved in a manner discussed by BFP and one may evaluate the D-waves in the threshold region and obtain the D-wave scattering lengths: however the availability of a parameteric representation of the three lowest waves essentially contains all the information required to compute these scattering lengths, with the higher wave and high energy contributions coming from the appropriate limits of the D-wave driving terms. The latter are not available in the literature which prevented a sharp evaluation of these scattering lengths that are correlated with a_0^0 in the range favored by standard chiral perturbation theory [14].

The purpose of this paper is to compute precisely such driving term con-

tributions to the D^- (and F^-) wave scattering lengths from the model of BFP. The D^- and F^- wave scattering lengths belong to a class of (combinations of) threshold parameters that are crucial in testing the predictions of chiral perturbation theory; as accurate a determination of such quantities as possible is therefore desirable. Since experimental numbers for these are in fact extracted from dispersion relation phenomenology, it is important to have a handle on the relative contributions of the low energy S - and P -waves and that of the medium and high energy tails to the relevant dispersion integrals.

In the following we will recall the basis of the dispersion relation analysis of Roy followed by a description of the BFP model, the details of which in Ref. [5, 6] are somewhat sketchy. The first step therefore is to reconstruct the BFP model; in order to establish the reconstruction we compute the S - and P -wave driving terms from the model, obtained from the appropriate Roy dispersion relations for amplitudes of definite isospin projected on these waves and compare them with the polynomial fits provided by BFP [5, 6]. Projecting on the D^- (F^-) wave, we obtain the corresponding D^- (F^-) wave driving terms: we will merely evaluate these in the threshold region which will yield the driving term contribution to the D^- (F^-) wave scattering lengths.

Indeed, it has been noted by BFP that crossing constraints are not guaranteed to be satisfied by this model. In order to test the reliability of this determination, we then compute the contributions of the medium and high energy information described by the model to three sets of a priori inequiv-

alent sum rules for these scattering lengths that are presently available in direct and indirect forms in the literature. These are obtained from considering (a) the Froissart-Gribov representation for the D-waves in the threshold region [4, 16], (b) those derived by Wanders [17], and (c) those derived from a system of sum rules presented by Ananthanarayan, Toublan and Wanders (ATW) [18]. We continue with a presentation of numerical details and a discussion of our results. Implications of this work to the results of Ref. [14] are discussed: in Ref. [14] only the resonance contributions of medium and high energy information were accounted for which contributed $0.54 \cdot 10^4$ ($0.43 \cdot 10^4$) to a_2^0 and $0.38 \cdot 10^4$ ($0.31 \cdot 10^4$) to a_2^2 with the Particle Data Group (BFP) parameters for the f_0 ; now the Regge and Pomeron contributions may also be included which are $1.40 \cdot 10^4$ to a_2^0 and $0.07 \cdot 10^4$ to a_2^2 respectively.

In two-loop chiral perturbation theory, parameters of the relevant effective lagrangian, enter the expressions for the two-loop predictions to the F-wave scattering length a_3^1 . We employ the fits to the Roy equations discussed in Ref. [14] to compute the S- and P-wave contributions to this important threshold parameter. In practice a_3^1 receives practically no contribution from the medium and high energy absorptive parts; this is established once more by computing the driving term contribution. Sum rules for a_3^1 (a) obtained from the appropriate limit of the Froissart-Gribov representation for the F-wave, and (b) obtained by ATW [19] are used to test the consistency of the

driving term contributions. In practice, these are found to be two orders of magnitude smaller than the contribution from the S- and P-waves.

2 Dispersion relations and Roy equations

The notation and formalism that we adopt in this discussion follows that of Ref. [6]. Consider scattering:

$$a(p_a) + b(p_b) \rightarrow c(p_c) + d(p_d);$$

where all the pions have the same mass, $m_\pi = 140 \text{ MeV}$ and is henceforth set equal to unity. [Unless explicitly mentioned all masses will be in the units of m_π .] The Mandelstam variables s , t and u are defined as

$$s = (p_a + p_b)^2; \quad t = (p_a - p_c)^2; \quad u = (p_a - p_d)^2; \quad s + t + u = 4; \quad (2.1)$$

The scattering amplitude $F(a; b \rightarrow c; d)$ (our normalization of the amplitude is that of Ref. [6], and differs from that of Ref. [9, 14] by 32π):

$$F(a; b \rightarrow c; d) = \frac{1}{2} A(s; t; u) + \frac{1}{2} A(t; s; u) + \frac{1}{2} A(u; t; s);$$

From $A(s; t; u)$ we construct the three s-channel isospin amplitudes:

$$\begin{aligned} T_s^0(s; t; u) &= 3A(s; t; u) + A(t; s; u) + A(u; t; s); \\ T_s^1(s; t; u) &= A(t; s; u) - A(u; t; s); \\ T_s^2(s; t; u) &= A(t; s; u) + A(u; t; s); \end{aligned} \quad (2.2)$$

One basis for the dispersion relation analysis of scattering data is dispersion relations for amplitudes of definite isospin in the s channel which may be written down with two subtractions (a number that guarantees convergence as a result of the Froissart bound, rigorously established in axiomatic field theory):

$$T_s^I(s; t; u) = \sum_{I^0=0}^2 C_{st}^{II^0} (C^{I^0}(t) + (s-u)D^{I^0}(t)) + \frac{1}{4} \int_{-1}^1 \frac{dx}{x^2} \left[\frac{s^2}{x-s} I^{II^0} + \frac{u^2}{x-u} C_{su}^{II^0} \right] A_s^{I^0}(x; t); \quad (2.3)$$

where $A_s^I(x; t)$ is the isospin I s channel absorptive part, C_{st} and C_{su} are the crossing matrices:

$$C_{st} = \begin{pmatrix} 0 & 1=3 & 1 & 5=3 \\ 1 & 1=3 & 1=2 & 5=6 \\ 1 & 1=3 & 1=2 & 1=6 \end{pmatrix} \begin{matrix} C \\ C \\ C \\ A \end{matrix}; \quad C_{su} = \begin{pmatrix} 0 & 1=3 & 1 & 5=3 \\ 1 & 1=3 & 1=2 & 5=6 \\ 1 & 1=3 & 1=2 & 1=6 \end{pmatrix} \begin{matrix} C \\ C \\ C \\ A \end{matrix}$$

and I is the identity matrix. Suppressing $u = 4 - s - t$ as an argument of T_s^I , we introduce the partial wave expansion:

$$T_s^I(s; t) = \sum_{l=0}^{\infty} (2l+1) P_l \left(1 + \frac{2t}{s-4}\right) f_l^I(s); \quad (2.4)$$

$$f_l^I(s) = \frac{1}{4} \int_{-1}^1 \frac{d^2 s}{s-0} dt T_s^I(s; t) P_l \left(1 + \frac{2t}{s-4}\right);$$

$$f_1^0(s) = f_1^2(s) = 0; \text{ odd}; \quad f_1^1(s) = 0; \text{ even}; \quad (2.5)$$

In terms of the phase shifts, δ_l^I , in the elastic region, we have:

$$f_l^I(s) = \frac{s}{s-4} \exp i \frac{\delta_l^I(s)}{4} \sin \frac{\delta_l^I(s)}{4}; \quad s \leq 16; \quad (2.6)$$

We also introduce the threshold expansion:

$$\text{Ref}_1^I(s) = \frac{s^4}{4} a_1^I + b_1^I \frac{s^4}{4} + \dots; s > 4; \quad (2.7)$$

where the a_1^I are the scattering lengths and the b_1^I are the effective ranges, namely the leading threshold parameters.

Roy eliminated the t -dependent unknown functions $C^I(t)$ and $D^I(t)$ in eq.(2.3) using crossing symmetry and Bose symmetry which implies: $C^1(t) = D^0(t) = D^2(t) = 0$, in favor of the S-wave scattering lengths. The result is the Roy form of the fixed t dispersion relations with two subtractions:

$$T_s^I(s;t) = \frac{1}{4} g_1^{II^0}(s;t) a_0^{I^0} + \frac{1}{4} \int_1^{I^0=0} ds^0 g_2^{II^0}(s;t;s^0) A_s^{I^0}(s^0;0) + g_3^{II^0}(s;t;s^0) A_s^{I^0}(s^0;t) \quad (2.8)$$

where the three functions $g_i^{II^0}$ listed in eq. (15)–(17) of Ref [1] are listed below:

$$\begin{aligned} g_1(s;t) &= s(I - C_{su}) + t(C_{st} - C_{su}) + 4C_{su}; \\ g_2(s;t;s^0) &= C_{st} \frac{I + C_{tu}}{2} + \frac{2s+t}{t} \frac{4I - C_{tu}}{4} \frac{1}{s^2} \\ &\quad - \frac{t^2 I}{s^0 t} + \frac{(4-t)^2 C_{su}}{s^0 (4+t)} - \frac{4tI + 4(4-t)C_{su}}{s^0 (4-t)}; \\ g_3(s;t;s^0) &= \frac{1}{s^2} \frac{s^2 I}{s^0 s} + \frac{(4-s-t)^2 C_{su}}{s^0 (4+s+t)} - \frac{(4-t)^2}{s^0 (4+t)} \\ &\quad - \left(\frac{C_{su} + I}{2} + \frac{2s+t}{t} \frac{4C_{su} - I}{2} \right); \end{aligned}$$

with $C_{tu}^{II^0} = (-1)^{I-II^0}$. The Roy equations are obtained upon projecting the resulting dispersion relation onto partial waves and inserting a partial wave

expansion for the absorptive part. They have been rigorously proved to be valid in the domain $4 \leq s \leq 60$. These are a system of coupled integral equations for partial wave amplitudes of definite isospin I which are related through crossing symmetry to the absorptive parts of all the partial waves.

The Roy equations for the S- and P-waves are [1, 2, 5, 6]:

$$\begin{aligned} f_0^0(s) &= a_0^0 + (2a_0^0 - 5a_0^2) \frac{s-4}{12} + \int_{I^0=0}^{I^0=1} \int_{I^0=0}^{I^0=1} \frac{dx}{x^2} K_{00}^{I^0 I^0}(s; x) \text{Im } f_{I^0}^{I^0}(x); \\ f_1^1(s) &= (2a_0^0 - 5a_0^2) \frac{s-4}{72} + \int_{I^0=0}^{I^0=1} \int_{I^0=0}^{I^0=1} \frac{dx}{x^2} K_{11}^{I^0 I^0}(s; x) \text{Im } f_{I^0}^{I^0}(x); \quad (2.9) \\ f_0^2(s) &= a_0^2 - (2a_0^0 - 5a_0^2) \frac{s-4}{24} + \int_{I^0=0}^{I^0=1} \int_{I^0=0}^{I^0=1} \frac{dx}{x^2} K_{20}^{I^0 I^0}(s; x) \text{Im } f_{I^0}^{I^0}(x) \end{aligned}$$

and for all the higher partial waves written as:

$$f_1^I(s) = \int_{I^0=0}^{I^0=1} \int_{I^0=0}^{I^0=1} \frac{dx}{x^2} K_{I1}^{I^0 I^0}(s; x) \text{Im } f_{I^0}^{I^0}(x); \quad I = 2;$$

where $K_{II}^{I^0 I^0}(s; s^0)$ are the kernels of the integral equations and whose explicit expressions have been documented elsewhere [2]. Upon cutting off the integral at a large scale and absorbing the contribution of the high energy tail as well as that of all the higher waves over the entire energy range into the driving terms $d_1^I(s; \infty)$ we have:

$$\begin{aligned} f_0^0(s) &= a_0^0 + (2a_0^0 - 5a_0^2) \frac{s-4}{12} + \int_{I^0=0}^{I^0=1} \int_{I^0=0}^{I^0=1} \frac{dx}{x^2} K_{00}^{I^0 I^0}(s; x) \text{Im } f_{I^0}^{I^0}(x) \\ &\quad + d_0^0(s; \infty); \\ f_1^1(s) &= (2a_0^0 - 5a_0^2) \frac{s-4}{72} + \int_{I^0=0}^{I^0=1} \int_{I^0=0}^{I^0=1} \frac{dx}{x^2} K_{11}^{I^0 I^0}(s; x) \text{Im } f_{I^0}^{I^0}(x) \end{aligned}$$

$$\begin{aligned}
& + d_1^1(s; \epsilon); \\
f_0^2(s) = & a_0^2 - (2a_0^0 - 5a_0^2) \frac{s-4}{24} + \sum_{l^0=0}^{\infty} \sum_{l^1=0}^{\infty} \int_4^{\infty} dx K_{20}^{l^0 l^1}(s; x) \text{Im} f_{l^0}^{l^1}(x) \\
& + d_0^2(s; \epsilon)
\end{aligned} \tag{2.10}$$

and for all the higher partial waves written as:

$$f_l^I(s) = \sum_{l^0=0}^{\infty} \sum_{l^1=0}^{\infty} \int_4^{\infty} dx K_{lI}^{l^0 l^1}(s; x) \text{Im} f_{l^0}^{l^1}(x) + d_l^I(s; \epsilon); \quad l-1 \leq l^1 \leq l+2:$$

From the following limits for the Roy equations

$$\lim_{s \rightarrow 4^+} \frac{\text{Re} f_2^0(s)}{((s-4)=4)^2}; \quad \lim_{s \rightarrow 4^+} \frac{\text{Re} f_2^2(s)}{((s-4)=4)^2}; \quad \lim_{s \rightarrow 4^+} \frac{\text{Re} f_3^1(s)}{((s-4)=4)^3} \tag{2.11}$$

we find expressions of sum rules for the D- and F-wave scattering lengths:

$$\begin{aligned}
a_2^0 = & \frac{16}{45} \int_4^{\infty} \frac{ds^0}{s^0(s^0-4)} \\
& \frac{1}{(s^0-4) \text{Im} f_0^0(s^0) + 9(s^0+4) \text{Im} f_1^1(s^0) + 5(s^0-4) \text{Im} f_0^2(s^0)} \\
& + \lim_{s \rightarrow 4^+} \frac{\text{Re} d_2^0(s; \epsilon)}{((s-4)=4)^2};
\end{aligned} \tag{2.12}$$

$$\begin{aligned}
a_2^2 = & \frac{16}{90} \int_4^{\infty} \frac{ds^0}{s^0(s^0-4)} \\
& \frac{1}{2(s^0-4) \text{Im} f_0^0(s^0) - 9(s^0+4) \text{Im} f_1^1(s^0) + (s^0-4) \text{Im} f_0^2(s^0)} \\
& + \lim_{s \rightarrow 4^+} \frac{\text{Re} d_2^2(s; \epsilon)}{((s-4)=4)^2};
\end{aligned} \tag{2.13}$$

$$\begin{aligned}
a_3^1 = & \frac{16}{105} \int_4^{\infty} \frac{ds^0}{s^0(s^0-4)} \\
& \frac{1}{2(s^0-4) \text{Im} f_0^0(s^0) + 9(s^0+4) \text{Im} f_1^1(s^0) - 5(s^0-4) \text{Im} f_0^2(s^0)} \\
& + \lim_{s \rightarrow 4^+} \frac{\text{Re} d_3^1(s; \epsilon)}{((s-4)=4)^3};
\end{aligned} \tag{2.14}$$

The objects of interest to us here are the driving terms $d_1^I(s; \epsilon)$ and in particular the driving term contributions to the D- and F-wave scattering

lengths

$$\lim_{s \rightarrow 4+} \frac{\text{Re } d_2^I(s; \gamma)}{((s-4)=4)^2}; \lim_{s \rightarrow 4+} \frac{\text{Re } d_3^I(s; \gamma)}{((s-4)=4)^3}$$

after the model for the medium and high energy contributions is pinned down. This will be discussed in the subsequent sections.

3 The BFP Model

The medium and high energy absorptive parts are described by BFP in terms of only one resonance, viz., the f_0 whose mass is taken to be $M_{f_0} = 1269$ MeV and elastic width to be $\Gamma_{f_0} = 125$ MeV. More updated information on this resonance may be obtained from [15], viz., $M_{f_0} = 1275$ MeV, $\Gamma_{f_0} = 185$ MeV, with the branching ratio of 85%, yielding an elastic width $\Gamma_{f_0} = 158$ MeV. We employ the BFP numbers since these have already gone into the driving terms for the S- and P-waves in the implementation of Ref. [14]. While details of the exact implementation are not available, we are faced with the option of representing this resonance in terms of say, a modified Breit-Wigner propagator along the lines of Pennington and Protopopescu [20] or merely in the narrow width approximation. In practice we have found that the contributions from the latter when added to the contributions arising from the remainder of the high energy model, yields good agreement with the published polynomial fit of BFP and we have chosen to work with it.

The expression for the absorptive part from the f_0 is therefore given by

$$A_s^0(s^0; t) = 5 \frac{s^0}{s^0 - 4} (s^0 - M_{f_0}^2) P_2(1 + 2t/(s^0 - 4)); 4 < s^0 < 1; \quad (3.1)$$

and $A_s^1(s^0; t) = A_s^2(s^0; t) = 0$.

BFP describe the high energy asymptotics in terms of (a) Pomeron exchange, and (b) Regge trajectory due to an exchange degenerate $+ f_0$ trajectory.

(a) Pomeron exchange: the BFP Pomeron is characterized by the logarithmic slope of the differential cross-section b , at an energy scale x_0 , with the slope of the Pomeron trajectory α_P^0 , and a total asymptotic cross-section, σ_1 . In terms of these, our reconstruction of the absorptive part in the $I = 0$, t -channel reads:

$$A_t^0(s^0; t) = \frac{3x_0}{32} \theta(z) e^{bt=2} \left(\frac{s^0}{x_0}\right)^{1+\alpha_P^0 t} (s^0 - 110); \quad (3.2)$$

while $A_t^1(s^0; t) = A_t^2(s^0; t) = 0$, and $\theta(z)$ is the step-function. This is obtained by suitably modifying the expressions for the absorptive parts presented in Ref. [20].

The BFP Pomeron is defined by the numerical choice, $b = 10 \text{ GeV}^{-2}$, $x_0 = 10 \text{ GeV}^2$, $\alpha_P^0 = 0.4 \text{ GeV}^{-2}$, $\sigma_1 = 1 \text{ mb} = 20 \text{ mb}$.

(b) Regge exchange: the BFP Regge trajectories are exchange degenerate $+ f_0$ poles whose residues are described by the Lovelace-Veneziano function

with universal coupling

$$\frac{f^2}{4} = 2.4:$$

BFP provide no further details of the Regge contributions. In order to reconstruct the above, we require the specification of the trajectory:

$$\alpha(t) = \frac{1}{2} + \frac{t}{2M^2}; \quad (3.3)$$

$M = 769 \text{ MeV}$. We then have the absorptive parts in the $I = 0; 1$ t -channels:

$$A_t^0(s^0; t) = A_t^1(s^0; t) = \frac{f^2}{16} \sin(\alpha(t)) (1=2 \quad \alpha(t)) \frac{s^0}{2M^2} \alpha(t) (s^0 \rightarrow 110); \quad (3.4)$$

and $A_t^2(s^0; t) = 0$.

In our numerical evaluation, we have chosen to work with (a) retaining upto the next to leading order contribution in $\frac{0}{p}$ since it is numerically small, and (b) the simplified Regge trajectory $\alpha(t) = 1=2$ since the Regge contributions are expected to be small and the retaining the slope of the trajectory entails higher order corrections in M^{-2} which are small.

4 S- and P - wave driving terms and D - wave scattering lengths

The relations eq.(3.1), (3.2) and (3.4) completely specify the BFP medium and high energy scattering model along with the crossing relation for the

s and t channel absorptive parts

$$A_s^I(s^0; t) = \sum_{I^0=0}^{X^2} C_{st}^{II^0} A_t^{I^0}(s^0; t); \quad (4.1)$$

and may be directly inserted into the dispersion relation (2.8) and then be subsequently projected onto the relevant partial waves, via. eq.(2.5). The results of the projection on to the S- and P- waves may be compared with the polynomial ts provided by BFP, [5, 6]. These are [BFP (I)]:

$$d_0^0(s) = 9.12 \cdot 10^4 (s - 4) + 9.78 \cdot 10^5 (s - 4)^2 \quad (4.2)$$

$$d_1^1(s) = 3.00 \cdot 10^5 (s - 4) + 2.30 \cdot 10^5 (s - 4)^2$$

$$d_0^2(s) = 7.20 \cdot 10^4 (s - 4) + 3.50 \cdot 10^5 (s - 4)^2$$

and [BFP (II)]:

$$d_0^0(s) = 9.12 \cdot 10^4 (s - 4) + 9.78 \cdot 10^5 (s - 4)^2 \quad (4.3)$$

$$d_1^1(s) = 1.36 \cdot 10^4 (s - 4) + 8.36 \cdot 10^6 (s - 4)^2 + 1.75 \cdot 10^7 (s - 4)^3$$

$$d_0^2(s) = 5.09 \cdot 10^4 (s - 4) + 6.32 \cdot 10^5 (s - 4)^2 - 3.78 \cdot 10^7 (s - 4)^3$$

The results are displayed in Fig. 1-3. An inspection shows that our reconstruction of the driving terms for these waves compares well with the BFP ts.

The results of the projection onto the D-waves when evaluated in the threshold region yields the D-wave driving term contribution to the D-wave scattering lengths. These are presented in Table 1.

Note that BFP [6] in their discussion of D-waves, redefine the driving terms in order to ensure normal threshold behaviour. We have not found the need to perform such a redefinition when we work with sufficiently high precision and since we are interested only in the scattering length and not in solving for the D-waves. Such a redefinition yields a contribution from the resonance of $2.7 \cdot 10^4$ for a_2^0 and 0 for a_2^2 in the narrow width approximation. We do not use these results any further.

We are now posed with the problem that the BFP model has not been explicitly required to respect crossing symmetry constraints. In order to test the reliability of this model we now compare the results obtained here with those from three sets of sum rules: Consider the Froissart-Gribov representation [4]:

$$f_1^I(t) = \frac{4}{(4-t)^4} \int_0^{Z_1} ds A_t^I(s^0; t) Q_1\left(\frac{2s^0}{4-t} - 1\right); l=2; \quad (4.4)$$

where $Q_1(z)$ is the standard Neumann symbol. The limit of this representation near threshold for $l=2$ yields the first set of sum rules for the D-wave scattering lengths and were also considered in a different context recently [16].

We find the "Froissart-Gribov sum rules":

$$a_2^I = \frac{1}{15} \int_0^{Z_1} \frac{d}{(s+1)^3} A_t^I(s^0; 4); \quad (4.5)$$

where $(s^0 - 4)=4$ is a convenient integration variable and in the physical region denotes the square of the centre of mass three momentum.

The second set were derived by Wanders by writing down dispersion relations for partially symmetric amplitudes in terms of partially symmetric homogeneous variables [17] which are reproduced below with our normalization and after eliminating some typographical errors:

$$a_2^0 = \frac{1}{45} \frac{Z_1}{0} \frac{d}{d} \frac{1}{(\epsilon + 1)^3} \frac{h}{A_s^0(\epsilon; 0) + 5A_s^2(\epsilon; 0) + \frac{3(\epsilon^2 + 3\epsilon + 1)}{2(\epsilon + 1)^3} A_s^1(\epsilon; 0)} \quad (4.6)$$

$$+ \frac{2}{(\epsilon(\epsilon + 1))^2} (4\epsilon + 3) \frac{\partial}{\partial t} A_s^0(\epsilon; 0) - 3 \frac{\partial}{\partial t} A_s^1(\epsilon; 0) + 5 \frac{\partial}{\partial t} A_s^2(\epsilon; 0) \quad ;$$

$$a_2^0 = \frac{1}{90} \frac{Z_1}{0} \frac{d}{d} \frac{1}{(\epsilon + 1)^3} \frac{h}{2A_s^0(\epsilon; 0) + A_s^2(\epsilon; 0) + \frac{3(\epsilon^2 + 3\epsilon + 1)}{2(\epsilon + 1)^3} A_s^1(\epsilon; 0)} \quad (4.7)$$

$$+ \frac{2}{(\epsilon(\epsilon + 1))^2} \left(2 \frac{\partial}{\partial t} A_s^0(\epsilon; 0) + 3 \frac{\partial}{\partial t} A_s^1(\epsilon; 0) + (7\epsilon + 6) \frac{\partial}{\partial t} A_s^2(\epsilon; 0) \right) \quad ;$$

where $\frac{\partial}{\partial t} A_s^I(\epsilon; 0) = \lim_{t \rightarrow 0} \frac{\partial}{\partial t} A_s^I(\epsilon; t)$. More recently ATW [18] considered certain totally symmetric amplitudes and obtained sum rules for various combinations of threshold parameters. Combining some of these and the Wanders sum rule for $18a_1^1 = 2a_0^0 + 5a_0^2$ [17], we obtain for the third set ("ATW sum rules") the following expressions:

$$a_2^0 = \frac{1}{45} \frac{Z_1}{0} \frac{d}{d} \frac{1}{(\epsilon + 1)^3} \frac{h}{A_s^0(\epsilon; 0) + 5A_s^2(\epsilon; 0) + \frac{3\epsilon^3 + 6\epsilon^2 + 2\epsilon + 2}{(\epsilon(\epsilon + 1))^3} A_s^1(\epsilon; 0)} \quad (4.8)$$

$$+ \frac{1}{(\epsilon(\epsilon + 1))^2} \left(\frac{18 + 20}{3} \frac{\partial}{\partial t} A_s^0(\epsilon; 0) + 4 \frac{\partial}{\partial t} A_s^1(\epsilon; 0) + \frac{40}{3} \frac{\partial}{\partial t} A_s^2(\epsilon; 0) \right) \quad ;$$

$$a_2^2 = \frac{1}{90} \frac{Z_1}{0} \frac{d}{d} \frac{1}{(\epsilon + 1)^3} \frac{h}{2A_s^0(\epsilon; 0) + A_s^2(\epsilon; 0) + \frac{3\epsilon^3 + 6\epsilon^2 + 2\epsilon + 2}{(\epsilon(\epsilon + 1))^3} A_s^1(\epsilon; 0)}$$

(4.9)

$$+ \frac{1}{(\ell(\ell+1))^2} \left[\frac{16}{3} \frac{\partial}{\partial t} A_s^0(\ell; 0) - 4 \frac{\partial}{\partial t} A_s^1(\ell; 0) + \frac{36+32}{3} \frac{\partial}{\partial t} A_s^2(\ell; 0) \right] :$$

The results of introducing eq.(3.1), (3.2) and (3.4) together with the crossing relation eq.(4.1) and the numerical choices of BFP documented in the previous section are displayed in Tables 2, 3 and 4 for the Froissart-Gribov (eq.(4.5)), Wanders (eq.(4.6) and (4.7)) and ATW (eq.(4.8) and eq.(4.9)) sum rules respectively. These may be viewed as tools that test the extent to which the results of Table 1 are reliable since the BFP model has not been required to satisfy crossing constraints. In the event crossing constraints were to be built into the model for medium and high energy scattering, the Roy equation driving term contributions would have to be identical to those obtained from any other system of sum rules.

We see that the entries of Table 1 are identical only to those of Table 3. This is ostensibly due to the manner in which the Roy equations and the Wanders' partially symmetric homogeneous variable technique implement crossing symmetry.

The numerical results of Table 4 are somewhat different from the above since these are based on dispersion relations written down for totally symmetric amplitudes in terms of totally symmetric homogeneous variables. Nevertheless, the results for the 0^+0^+ combination

$$a_2 = a_2^0 + 2a_2^2$$

is identical for the entries of Table 1, 3 and 4. This is not unexpected since the Roy equations, Wanders and ATW sum rules all involve only physical region quantities, viz., at the physical point $t = 0$. This is not so even for a_2 from the Froissart-Gribov sum rules, which requires the evaluation of quantities at the unphysical point $t = 4$.

Special attention may however be paid to the Regge contribution to a_2 in Tables 1-4 which are identical. This results from the fact that with the simplified Regge trajectory $\alpha(t) = 1/2$, the Regge contribution to the absorptive parts have no t dependence; a pure S- (and P-) wave contribution will automatically satisfy crossing constraints derived from dispersion relations with two subtractions and crossing symmetry is recovered by the decoupling of the $I = 1$ channel.

The Pomeron contributions are approximately equal for all the 4 evaluations of a_2 since the absorptive parts are dominated by S- and P-wave contributions with corrections coming from higher waves. The resonance contributions from the Froissart-Gribov representation to a_2 differ appreciably from the contributions computed from physical region sum rules reflecting an unsatisfactory representation of the absorptive parts due to the $l=2$ resonance exchange, say at the level of about 30%. Nevertheless, in toto the model yields answers for a_2^0 and a_2^2 that always remain comparable, allowing us to judge the BFP model as being fair in its implementation of crossing symmetry.

We finally remark on the numerical impact of this work are to the results of the recent analysis of data [14]. The resonance contributions of medium and high energy information which contributed $0.54 \cdot 10^4$ to a_2^0 and $0.38 \cdot 10^4$ to a_2^2 with the Particle Data Group parameters for the f_0 were presented there. The numerical details with the BFP parameters for the f_0 are now presented in Tables 1-4 and also available are the Regge and Pomeron contributions may also be included which yield $1.40 \cdot 10^4$ to a_2^0 and $6.82 \cdot 10^6$ to a_2^2 . In Table 5 we present our results for a_2^0 and a_2^2 for the Roy equations discussed in our earlier work [14], explicitly accounting for the S- and P-wave contributions and driving term contributions. The total contribution of the medium and high energy absorptive parts is thus seen to be an important fraction of the central experimental value for a_2^0 quoted to be $17 \cdot 10^4$ by Nagels et al. [7]. When this is now completely accounted for, the results of our recent work [14] revise our numbers into the neighbourhood of this number, from the neighbourhood of $15 \cdot 10^4$. Our conclusions on a_2^2 vis a vis our earlier work are not significantly changed since the Regge and Pomeron contribution here is about 25% of the contribution of the resonance.

5 The F-wave scattering length a_3^1

In the previous section we have considered the implications of the medium and high energy scattering information to the D-wave scattering lengths

that receive contributions in chiral perturbation theory from parameters in the Lagrangian introduced at order p^4 [9]. The F-wave scattering length a_3^1 received contributions at order p^4 from pure loop contributions and would be significantly modified at the next order in chiral perturbation theory [11, 12]. This receives contributions from the S- and P-wave phase shifts from dispersive relations that might be written down for the $I = 1, l = 3$ F-wave and also from the medium and high energy parts. The former were not considered in Ref. [14] since at that point only phenomenological parameters at one-loop were considered. However, we will use this opportunity to compute the medium and high energy contributions to the F-wave scattering length, as well as the S- and P-wave contributions. In Table 6 we provide the S- and P-wave contributions to a_3^1 from the Roy equations for $\text{Im } f_0^0(s^0)$, $\text{Im } f_0^2(s^0)$ and $\text{Im } f_1^1(s^0)$, employed in Ref. [14], upon inserting these into the ds^0 integral in eq.(2.14).

Once more, the Roy equations contributions of the medium and high energy absorptive parts may be used by employing the relations eq.(3.1), (3.2) and (3.4) and may be inserted into the dispersion relation (2.8) and then be subsequently projected onto the $I = 1, l = 3$ partial wave, via. eq.(2.5). We may once again consider the Froissart-Gribov representation eq.(4.4) for the F-wave and consider it in the threshold region, which yields

the sum rule:

$$a_3^1 = \frac{1}{70} \int_0^{\infty} \frac{d}{(t+1)^4} A_t^1(\cdot; 4) \quad (5.1)$$

Another sum rule for this quantity has been obtained by Ananthanarayan, Toublan and Wanders [19] from techniques of the kind described in [17, 18] and is given below :

$$\begin{aligned} a_3^1 = & \frac{1}{420} \int_0^{\infty} \frac{d}{(t+1)^4} \left[2A^0(\cdot; 0) - 5A^2(\cdot; 0) + \frac{3(t+2)}{2} A^1(\cdot; 0) \right. \\ & + \frac{4}{(t+1)^3} \frac{\partial}{\partial t} (2A^0(\cdot; 0) - 5A^2(\cdot; 0)) + \frac{48}{2(t+1)^3} (t^2 + 4t + 2) \\ & \left. \frac{\partial}{\partial t} \frac{A^1(\cdot; 0)}{2t+4} \right] : \end{aligned} \quad (5.2)$$

The BFP absorptive parts for the medium and high energy parts may be inserted into each of these sum rules and in Table 7 we provide a compilation of the numbers of interest. We note that the resonance contributions to the Froissart-Gribov and ATW sum rules are identical: this is not a numerical coincidence; one may show that insertion of eq.(3.1) in eq.(5.1) and eq.(5.2) yields identical expressions. The Pomeron yields a contribution numerically comparable to that of the resonance only in case of the Roy equations, reflecting a breakdown of the model. Nevertheless, the medium and high energy contribution is 2 orders of magnitude lower than that of the S- and P-wave contribution.

Indeed in Ref. [18] it was pointed out that the sum rule for a_3^1 belongs to a family of such rapidly converging ones that it is fair to expect the contribution from the medium and high energy tail to be small in comparison with that

from the low energy S- and P-wave contributions. An inspection of Tables 6 and 7 indeed bears out this expectation. It may be concluded from Tables 6 and 7, that when Roy equations to scattering data is performed with $a_0^0 = 2(0.19; 0.21)$, the result for $a_3^1 = (4.2 \pm 0.2) \cdot 10^5$, which is compatible with the numbers presented in Ref. [7]. The one-loop chiral prediction for this quantity is $2 \cdot 10^5$ [9] and a substantial revision of this due to two-loop effects is entirely reasonable.

Acknowledgments

We thank the Swiss National Science Foundation for support during the course of this work. It is a pleasure to thank H. Leutwyler for discussions and crucial insights. We thank M. R. Pennington for having brought Ref. [20] to our attention.

References

- [1] S. M. Roy, Phys. Lett. B 36 (1971) 353.
- [2] J. L. Basdevant, J. C. Le Guillou and H. Navelet, Nuovo Cimento 7 A (1972) 363.
- [3] See, e. g., A. Martin, "Scattering Theory: Unitarity, Analyticity and Crossing," Springer-Verlag, Berlin, Heidelberg, New York, 1969.

- [4] B. R. Martin, D. Morgan and G. Shaw, "Pion-Pion Interaction in Particle Physics," Academic Press, London/New York, 1976.
- [5] J. L. Basdevant, C. D. Froggatt and J. L. Petersen, Phys. Lett. 41B (1972) 173; *ibid* 178.
- [6] J. L. Basdevant, C. D. Froggatt and J. L. Petersen, Nucl. Phys. B 72 (1974) 413.
- [7] M. M. Nagels et al., Nucl. Phys. B 147 (1979) 189.
- [8] See, e.g., H. Leutwyler, Ann. Phys. (N.Y.) 235 (1994) 165.
- [9] J. Gasser and H. Leutwyler, Ann. Phys. (N.Y.) 158 (1984) 142.
- [10] See e.g., M. Knecht and J. Stern, The Second DA NE Physics Handbook, L. Maini, G. Pancheri and N. Paver, eds., INFN Publication (1995), 169.
- [11] M. Knecht, B. Moussallam, J. Stern and N. H. Fuchs, Nucl. Phys. B 457 (1995) 513; M. Knecht, B. Moussallam, J. Stern and N. H. Fuchs, hep-ph/9512404.
- [12] J. Bijnens, G. Colangelo, G. Ecker, J. Gasser and M. Sainio, hep-ph/9511397.

- [13] See, e.g., J. Stem, H. Sazdjian and N. H. Fuchs, Phys. Rev. D 47 (1993) 3814; B. Ananthanarayan, D. Toublan and G. W. anders, Phys. Rev. D 51 (1995) 1093.
- [14] B. Ananthanarayan and P. Buttiker, hep-ph/9601285.
- [15] Particle Data Group, L. Montanet et al., Phys. Rev. D 73 (1994) 1173.
- [16] M. R. Pennington and J. Portoles, Phys. Lett. B 344 (1995) 399.
- [17] G. W. anders, Helv. Phys. Acta 39 (1966) 228.
- [18] B. Ananthanarayan, D. Toublan and G. W. anders, hep-ph/9510254.
- [19] B. Ananthanarayan, D. Toublan and G. W. anders, unpublished.
- [20] M. R. Pennington and S. D. Protopopescu, Phys. Rev. D 7 (1973) 2591.

Figure Captions

Fig. 1. Plot of $d_0^0(s;110)$ vs. s for $4 \leq s \leq 60$; solid line corresponds to our result, dashed line to the polynomial tBFP (I) from [5] and dots to the polynomial tBFP (II) from [6]. [Note that for the $I = 0$ S-wave the two polynomial ts of BFP are the same].

Fig. 2. As above for $d_1^1(s;110)$.

Fig. 3. As above for $d_0^2(s;110)$.

Table C options

Table 1. Contributions to a_2^0 , a_2^2 and a_2 from resonance, Pomeron exchange and Regge trajectories extracted from the Roy equations.

Table 2. As Table 1 but extracted from the Froissart-Gribov representation.

Table 3. As Table 1 but extracted from the Wanders sum rules.

Table 4. As Table 1 but extracted from the ATW sum rules.

Table 5 (a). Contributions to a_2^0 from the S- and P-wave Roy equation solutions of Ref. [14], driving term contributions and their sum, (b) As in (a) for a_2^2 .

Table 6. Contributions to a_3^1 from the S- and P-wave Roy equation solutions of Ref. [14]. [Note that the medium and high energy contributions are negligible in comparison.]

Table 7. Contributions to the $I = 1, l = 3, F$ -wave scattering length a_3^1 from the resonance, Pomeron exchange and Regge trajectories extracted from the Roy equations, Froissart-Gribov sum rule and the ATW sum rule.

	Resonance	Pomeron	Regge	Total
a_2^0	$4.33 \cdot 10^5$	$1.06 \cdot 10^4$	$2.84 \cdot 10^5$	$1.78 \cdot 10^4$
a_2^2	$3.01 \cdot 10^5$	$1.10 \cdot 10^5$	$7.58 \cdot 10^7$	$4.03 \cdot 10^5$
a_2	$10.35 \cdot 10^5$	$1.28 \cdot 10^4$	$2.69 \cdot 10^5$	$2.59 \cdot 10^4$

Table1

	Resonance	Pomeron	Regge	Total
a_2^0	$3.43 \cdot 10^5$	$1.26 \cdot 10^4$	$2.69 \cdot 10^5$	$1.88 \cdot 10^4$
a_2^2	$3.43 \cdot 10^5$	0	0	$3.43 \cdot 10^5$
a_2	$10.29 \cdot 10^4$	$1.26 \cdot 10^4$	$2.69 \cdot 10^9$	$2.57 \cdot 10^4$

Table2

	Resonance	Pomeron	Regge	Total
a_2^0	$4.33 \cdot 10^5$	$1.06 \cdot 10^4$	$2.84 \cdot 10^5$	$1.78 \cdot 10^4$
a_2^2	$3.01 \cdot 10^5$	$1.10 \cdot 10^5$	$7.58 \cdot 10^7$	$4.03 \cdot 10^5$
a_2	$10.35 \cdot 10^5$	$1.28 \cdot 10^4$	$2.69 \cdot 10^5$	$2.59 \cdot 10^4$

Table3

	Resonance	Pomeron	Regge	Total
a_2^0	4.05 10^5	1.13 10^4	2.78 10^5	1.81 10^4
a_2^2	3.15 10^5	7.32 10^6	4.96 10^7	3.83 10^5
a_2	10.35 10^5	1.28 10^4	2.69 10^5	2.59 10^4

Table 4

a_0^0	S- and P -	Driving term	Total
0.19	14.1 10^4	1.8 10^4	15.9 10^4
0.20	14.1 10^4	1.8 10^4	15.9 10^4
0.21	14.2 10^4	1.8 10^4	16.0 10^4

Table 5 (a)

a_0^0	S- and P -	Driving term	Total
0.19	0.18 10^4	0.40 10^4	0.58 10^4
0.20	0.29 10^4	0.40 10^4	0.69 10^4
0.21	0.41 10^4	0.40 10^4	0.81 10^4

Table 5 (b)

a_0^0	a_3^1
0.19	4.1 10^5
0.20	4.2 10^5
0.21	4.4 10^5

Table 6

	Resonance	Pomeron	Regge	Total
Roy equation	3.14 10^7	4.16 10^7	1.34 10^7	8.64 10^7
Froissart Gribov	3.58 10^7	0	1.26 10^7	4.84 10^7
ATW	3.58 10^7	1.77 10^9	1.25 10^7	4.85 10^7

Table 7

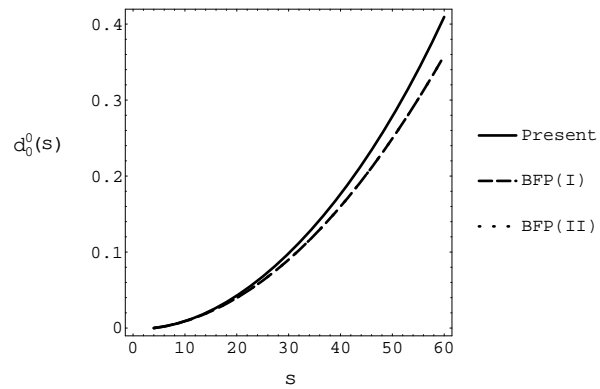


Fig. 1

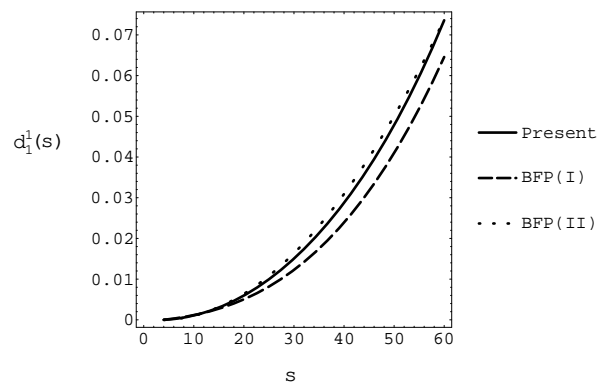


Fig. 2

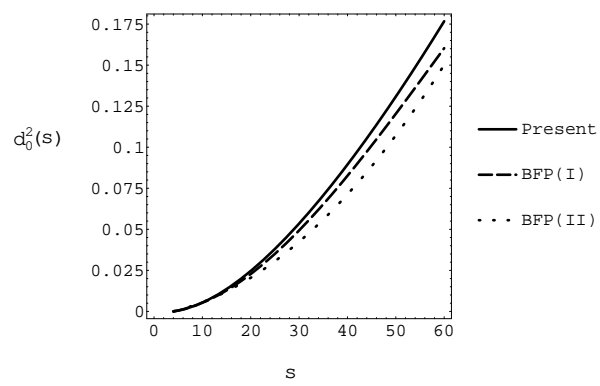


Fig. 3